SCIENTIFIC PAPERS
OF THE UNIVERSITY OF PARDUBICE
Series A
Faculty of Chemical Technology
3 (1997)

CHARGE TRANSFER ACROSS THE INTERFACE BETWEEN TWO IMMISCIBLE ELECTROLYTE SOLUTIONS AND ANALYTICAL APPLICATIONS

Hailemichael ALEMU[a1], Theodros SOLOMON[a], Bernd HUNDHAMMER[a], Kurt KALCHER[b] and Klemens SCHACHL[b]
[a]Department of Chemistry, Addis Ababa University, PO BOX 1176, Addis Ababa, Ethiopia
[b]Institute of Analytical Chemistry, Karl-Franzens University, A-8010 Graz

Received September 12, 1997

The transfer of several ions across the water/2-chloroethyl ether and water/o-dichlorobenzene interfaces has been investigated by DC and AC cyclic voltammetry. The standard Gibbs energies of ion transfer have been determined based on the tetraphenylarsonium tetraphenylborate assumption. The results have been compared with theoretical data calculated from an ionic solvation model. The transfer of transition metal-terpyridine complexes across the water/nitrobenzene interface has also been studied and from the voltammetric measurements the standard Gibbs energies of transfer have been evaluated. An amperometric detector based on membrane stabilized interface between two immiscible electrolyte solutions has been developed. It has been tested in a flow injection system for the determination of anions and cations. The detection limit of the detector has been determined to be about 5 x 10^{-7} M for the ions studied.

[1] To whom correspondence should be addressed

Introduction

The investigation of ion transfer across two immiscible electrolyte solutions (ITIES) has attracted a great deal of interest [1-4]. The importance and applications of such work in the fields of chemistry and biology have been described in several review articles [3,4]. The transfer of ions from one solvent to another is of particular interest to chemists dealing with diverse problems such as phase transfer catalysis in organic synthesis, solvent extraction in hydrometallurgy and electroanalytical chemistry [5]. Thermodynamic quantities for individual ionic species can also be obtained from such experiments.

Voltammetry at the interface of two immiscible electrolyte solutions has been the subject of considerable interest [6] and has shown promise as an analytical method. This concept extends electrochemical research into another class of substances that may not undergo electron transfer at the electrode/electrolyte interface. The determination of a variety of electroinactive ions that can transfer across the liquid/liquid interface has become possible by means of direct electroanalysis [7]. On the other hand the voltammetry of metal ions that are not transferable at ITIES can be studied by facilitating their transfer using mediators (neutral ionophores) in the organic phase or the transfer of the metal ions complexed with suitable organic ligands [8-10]. Due to the requirements of high dielectric constant ($\geq$ 10), immiscibility with water and different density from that of water, few organic solvents have been used so far, mainly nitrobenzene and 1,2-dichloroethane. Extending the studies to other solvents is hindered by the fact that most of the general organic solvents either are miscible with water or have low dielectric constant. Therefore searching for new solvents and supporting electrolytes for the organic phase is an attractive topic in this field.

The stabilization of the liquid/liquid interface by the insertion of porous membranes (either hydrophilic or lipophilic) has been successfully used to construct liquid state ion-selective electrodes (IES) [11]. The membrane-stabilised liquid/liquid interface has also been utilized as an amperometric sensor for the analytical determination of several ions in drinking water and foods [12]. Electrochemical investigations of ion transfer across these interfaces have yielded additional information about membrane diffusion coefficients [13].

The aim of this paper is to show the studies made on simple ion transfer, facilitated ion transfer, and complex ion transfer across the water/organic solvent systems and membrane-stabilised interface of two immiscible electrolyte solutions and the possible use of the method for analytical application.

Experimental

Studies of the simple ion and complex ion transfer across the immiscible electrolyte solution interfaces were carried out using a four electrode potentiostat

with iR compensation. For the ac cyclic voltammetric investigations, the current output of the potentiostat was connected to the input of a lock-in analyser (PAR Model 5204). The superimposed sinusoidal potential was of magnitude ΔE = 5 mV, peak to peak. Both the ac and the dc cyclic voltammetric techniques employed in these works were similar to those described in [14]. Ag/AgCl and saturated calomel electrodes were used as the reference electrodes in the organic and aqueous solutions, respectively. The anions NO_3^- and ClO_4^- were used as internal standards to fix the Galvani potential differences. The electrochemical cell used for the ion transfer gave an interfacial area of 0.69 cm^2.

Figure 1 shows the scheme of the experimental set-up used for the flow injection system of the membrane stabilised interface and the wall-jet electrochemical cell employed.

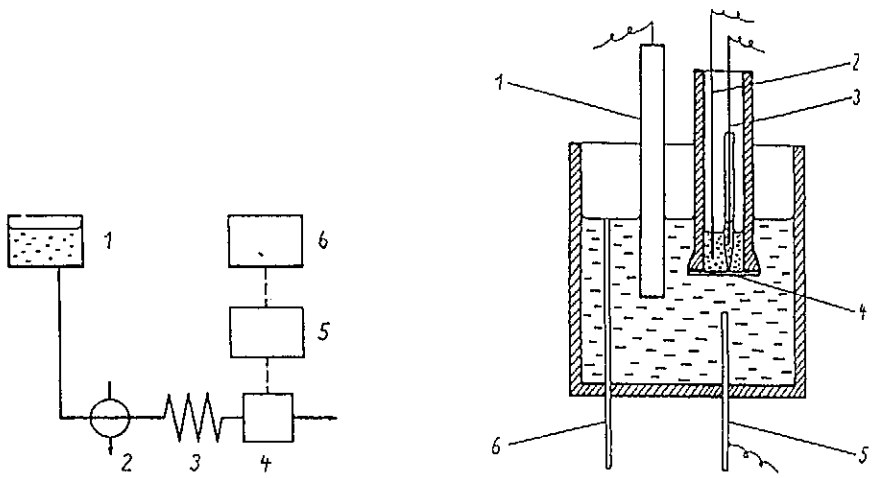

Fig. 1 (a) Block diagram of the flow-injection system: 1 reservoir of the carrier solution, 2 sample loop, 3 mixing coil, 4 detector, 5 four-electrode potentiostat, 6 *y-t* recorder. (b) Wall-jet cell: 1, 3 reference electrodes, 2 counter electrode in the organic phase, 4 membrane, 5 jet inlet (stainless steel needle) serves as counter electrode, 6 outlet

A hydrophobic poly(ethylene terephthalate) membrane (PETP-membrane) (Rossendorf Germany) was used to stabilize the water/nitrobenzene interface. The thickness of the membrane was 10 μm. A disk of this membrane, 1.3 cm in diameter was glued on to a glass tube (0.6 to 0.9 cm inner diameter) with epoxy resin. The glass tube was filled with 0.5 cm^3 of a 10 mM solution of the organic supporting electrolyte solution.

The base electrolytes used in the aqueous phase were 10 mM LiCl (Aldrich), 5 mM Li_2SO_4 (Fluka), 10 mM LiF (Aldrich). For the flow injection system, either a 7.5 mM LiH_2PO_4 (Aldrich) or a 5 mM Na_2SO_4 (Aldrich) solution was used as the supporting electrolyte and carrier solution. The base electrolytes employed in the organic phase were 10 mM tetraphenylarsonium

tetrakis(4-chlorophenyl) borate (TPAsTPBCl), 10 mM μ-nitridobis- (triphenylphosphorus)3,3-como-bis(undecahydro-1,2-dicarba-3-cobalt-closo-dodecabor)ate (PNPDCC). To fix the zero of the Galvani potential difference of the interface, the ionic transfer of tetraphenylarsonium tetraphenylborate (TPAsTPB) was used as described in Ref. [14]. Nitrobenzene (>99%; Aldrich) and 2-chloroethyl ether (>99%; Fluka) were used without further purification. *o*-Dichlorobenzene (99%; Aldrich) was distilled in vacuum and only the middle fraction was used for the experiments. All the chemicals used were of analytical grade and the aqueous electrolyte solutions were prepared from all glass doubly-distilled water. The organic and the aqueous phase were equilibrated with each other before use. All measurements were carried out at laboratory temperature (22 ± 1 °C).

Results and Discussion

(i) Ion Transfer across the Water/2-chlorethyl Ether and the Water/o-dichlorobenzene Interfaces

Figure 2 compares the dc voltammograms of the base electrolytes obtained at the water/2-chloroethyl ether interface for 10 mM LiCl in the aqueous phase and 10 mM TPAsTPB (a), TPAsTPBCl (b) and PNPDCC (c) in the organic phase. As it can be seen from the figure, the largest potential window is observed for the electrolyte couple LiCl(w)/PNPDCC(o). The polarization range obtained is reasonably wide to detect the transfer of many ions which have been previously studied at the water/nitrobenzene or water/1,2-dichloroethane interface.

Figure 3 shows the dc voltammograms for the transfer of SCN^- and methylviologen (MV^{2+}) ions from water to organic phase and back to water. The reversibility of the ion transfer was checked from the 59/Z mV (z = ionic charge) peak to peak separation. This was also apparent from the sweep rate (2–200 $mV\,s^{-1}$) and concentration (0.01–0.1 mM) independence of the peak potentials.

The plots of the peak currents versus the square roots of the sweep rates for the transfer of the studied ions showed linear dependence and from the slopes of the plots the diffusion coefficients of the ions in water were obtained using the Randes-Sevick equation [15]. The standard Galvani potential differences $\Delta^w{}_o\Phi^o$ were determined from the half-wave potentials $\Delta^w{}_o\Phi^o_{1/2}$ of the voltammograms using the following equation [15].

$$\Delta^w{}_o\Phi^o_{1/2} = \Delta^w{}_o\Phi^o + \frac{RT}{zF}\ln\left(\frac{D_w}{D_o}\right)^{1/2}\frac{\gamma_o}{\gamma_w} \qquad (1)$$

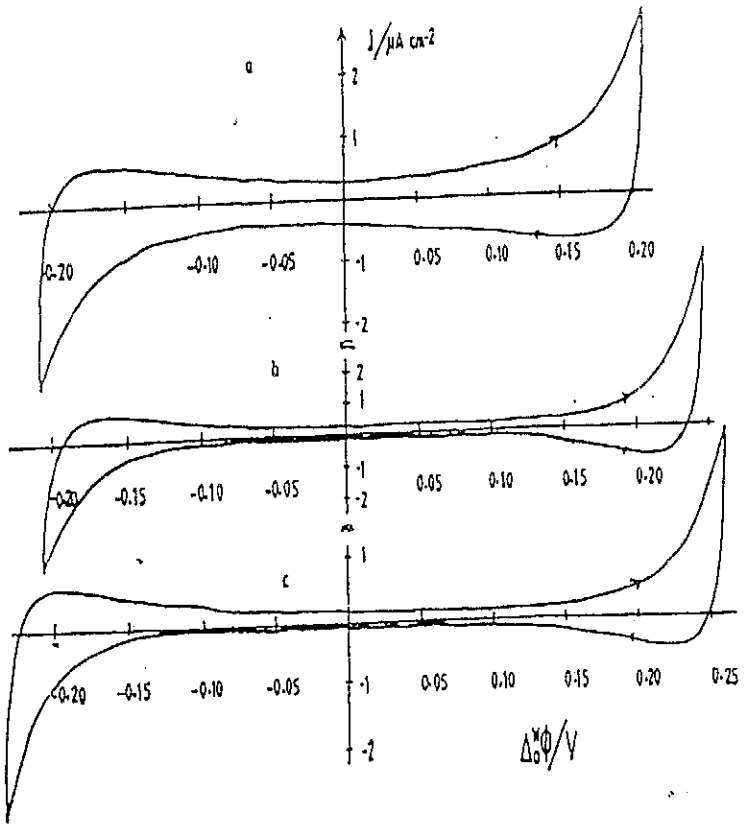

Fig. 2 Comparison of the cyclic voltammograms of 10 mM LiCl in water and 10 mM TPAsTPB (a), TPAsTPBCl (b), PNPDCC (c) in 2-chloroethyl ether at a sweep rate of 10 mV s^{-1}

Where D_w and D_o are the diffusion coefficients of the ions in the aqueous and the organic phase respectively, and γ_w and γ_o are the activity coefficients in the respective phases. The standard Gibbs energies of transfer of the ions $\Delta G_t^{o(w\rightarrow o)}$ were determined from the values of the standard Galvani potential difference [15]. Theoretical $\Delta G_t^{o(w\rightarrow o)}$ values of the ions were calculated employing the ion solvation model of Abraham, and Liszi [16,17]. A comparison of the experimental and the theoretical results of $\Delta G_t^{o(w\rightarrow o)}$ is presented in Table I.

As it seen from the table, the solvation state of the ions during the transfer process can be analyzed by comparing the experimental with the theoretical $\Delta G_t^{o(w\rightarrow o)}$ values. The experimental results of tetramethylammonium (TMA^+), tetraethylammonium (TEA^+), SCN^- and picrate (Pi^-) lie between the two theoretical extreme values which were calculated for fully hydrated ions in the organic phase. This implies that these ions are probably transferred partially hydrated. On the other hand tetrapropylammonium ($TPrA^+$), tetrabutyl-ammonium (TBA^+), ClO_4^- and IO_4^- have experimental $\Delta G_t^{ow\rightarrow o}$ values which

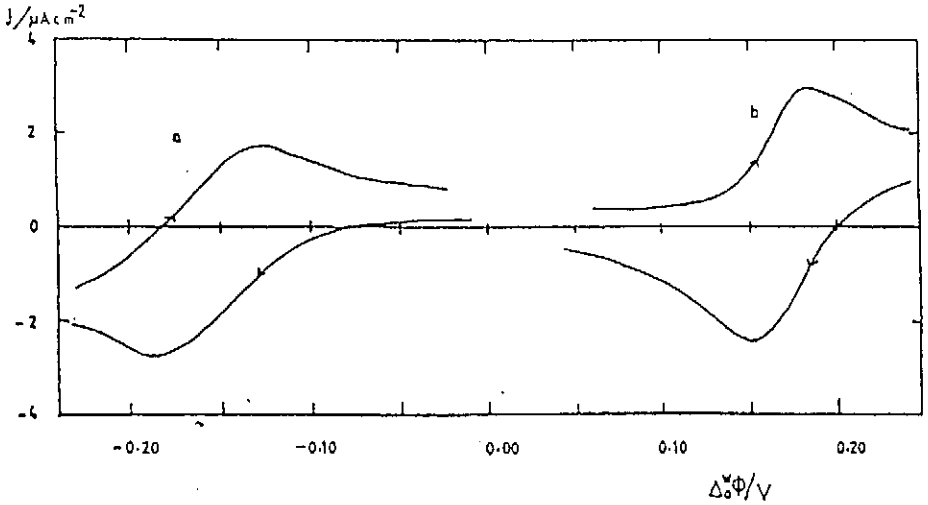

Fig. 3 Cyclic voltammetry for the transfer of SCN^- and MV^{2+} from water to the organic phase and back. Base electrolytes: 10 mM LiCl (aq) and 10 mM TPAsTPBCl (o), sweep rate = 20 mV s^{-1}

Table I Comparison of the experimental and theoretically calculated values of standard Gibbs energies of transfer of selected ions from water to 2-chloroethyl ether

Ion	ΔG_t^o, kJ mol^{-1}		
	Exp.	Theor.	
		(a)	(b)
$TMeA^+$	11.8	22.1	2.1
$TEtA^+$	4.3	9.6	-6.7
$TPrA^+$	-4.9	-4.2	-18.2
$TBuA^+$	-16.1	-17.9	-30.4
ClO_4^-	7.1	11.9	-15.9
IO_4^-	9.6	9.8	-10.5
SCN^-	17.2	34.0	7.4
Pi^-	-3.1	3.4	-13.5

(a) Calculated for non-hydrated ions in the organic phase
(b) Calculated for fully-hydrated ions in the organic phase

are very close to the theoretical calculated values for non-hydrated ions in the organic phase. These observations are in agreement with the general prediction that can be made by taking only the size of the ions into consideration. Some of the factors which cause the co-transfer of H_2O molecules with ions into

organic solvents are the aggregation of the organic electrolyte into ion-pairs, change of the nature of the organic medium by the organic salt followed by an increase in its water uptake and the formation of hydrogen bonds [18]. In this study, however, the first two effects have been minimized since the concentrations of the electrolytes were restricted to less than or equal to, 10 mM and the dielectric constant of the organic solvent is high enough to dissociate the electrolytes completely. Therefore it appears that the observed enhancement in the partial hydration of the transferred ions may be due to hydrogen bond formation between transferred water of hydration and the ether functionality in the solvent molecules.

The potential window of the water/*o*-dichlorobenzene interface obtained with PNPDCC is wide enough to investigate the transfer of even relatively hydrophilic ions like NO_3^- and ClO_3^- by dc and ac cyclic voltammetry. Figure 4 shows a typical ac cyclic voltammogram from which the half-wave potentials of the ions investigated were obtained from the peak potentials.

All dc cyclic voltammetric criteria, such as the separation of the peak potentials by about 60 mV, their independence of the sweep rate up to 100 mV s^{-1} and the dependence of the peak current on square root of the sweep rate indicate that the ion transfer across the water/*o*-dichlorobenzene interface is diffusion controlled at low sweep rates. The diffusion coefficient of PF_6^- in

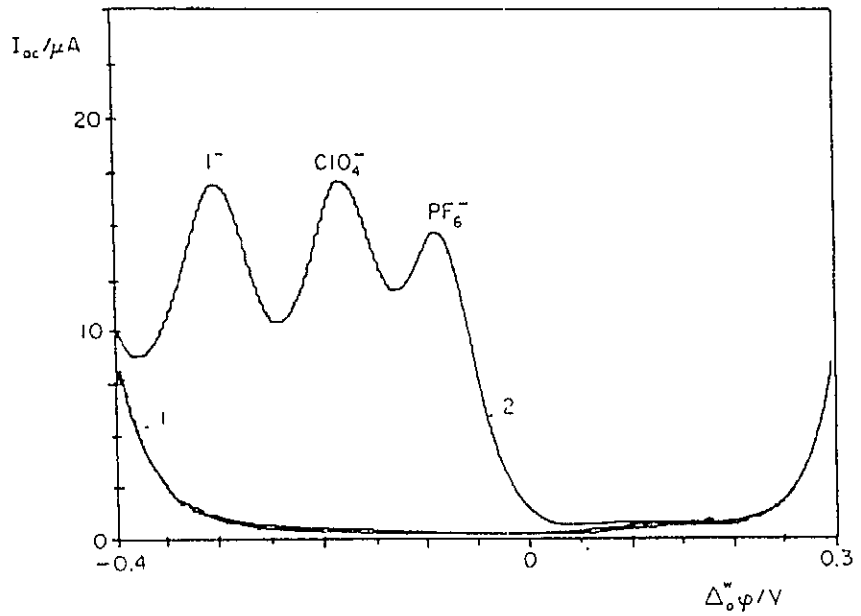

Fig. 4 Ac cyclic voltammogram at water/*o*-dichlorobenzene interface: Supporting electrolytes 5×10^{-3} M Li_2SO_4 (water) and 10^{-2} M PNPDCC (*o*-DCB). Curve 1 - supporting electrolyte only, curve 2 - after addition of NH_4PF_6, $LiClO_4$ and NaI at concentration of 10^{-4} M. f = 35, E_{ac} = 10 mV, sweep rate = 10 mV s^{-1}

water obtained from the plot of the peak potential as a function of the square root of the sweep rate (D = 1.4×10^{-5} $cm^2 s^{-1}$) agrees fairly well with the diffusion coefficient of PF_6^- calculated from the molar conductance of the ion at infinite dilution (D_o = 1.57×10^{-5} $cm^2 s^{-1}$) [19]. The half-peak width of the ac voltammetric peaks is 90 mV, and the forward and backward scans coincide at low ac frequencies; this can be taken as a further criterion for the diffusion control of the ion transfer. The values of the standard Galvani potential difference of the ions were determined by taking into account the ion association in the organic phase. The experimental results with the values of the theoretical standard Gibbs transfer energies are listed in Table II. The good agreement of the calculated values which are obtained assuming that the non-hydrated ion exists in the organic phase underlines the capability of this simple model to obtain estimates of Gibbs transfer energies.The plot of ΔG_t° (water/1,2-dichloro-

Table II Half-wave potentials and standard Gibbs energies of transfer of ions from water to *o*-dichlorobenzene

Ion	$\Delta^w{}_o\Phi^\circ_{1/2}$, V	$\Delta^w{}_o\Phi^\circ$, V	ΔG_t°, kJ mol^{-1} (Exp.)	ΔG_t°, kJ mol^{-1} (Theor.)[a]
$TPAs^+$	-0.316	-0.273	-26.30	
$TPtA^+$	-0.323	-0.283	-27.30	-28
$TBuA^+$	-0.177	-0.131	-12.60	-15
$TPrA^+$	-0.080	-0.032	-3.10	-1
$TEtA^+$	0.067	0.116	11.20	13
$TMeA^+$	0.226	0.277	26.73	26
I^-	-0.319	-0.406	39.20	
ClO_4^-	-0.182	-0.266	25.70	
MnO_4^-	-0.129	-0.208	20.10	
BF_4^-	-0.248	-0.332	32.00	
BF_6^-	-0.088	-0.165	15.90	
Pi^-	-0.049	-0.135	13.00	
SCN^-	-0.285	-0.369	35.60	
NO_3^-	-0.389	-0.489	47.20	
ClO_3^-	-0.375	-0.468	45.20	
TPB^-	-0.316	0.273	26.30	

[a]Calculated according to Abraham and Liszi [16] for non-hydrated ions in the organic phase

ethane) [20] versus ΔG_t° (water/*o*-dichlorobenzene) showed a very good correlation (r = 0.997) with a slope very close to unity. This is in agreement with the linear Gibbs energy relationship proposed by Solomon [21].

(ii) Transition Metal-terpyridine Complexes Transfer across the Water/ nitrobenzene Interface

Figure 5 shows the ac and dc cyclic voltammograms of the supporting electrolyte and of an air-saturated solution of Co-terpyridine in a 5:1 metal to ligand ratio. No transfer of the uncomplexed metal cation was observed in the absence of the complexing agent.

As it can be seen from both voltammograms, three kinds of charged species are transferred reversibly across the interface. From the ac voltammogram of the in-phase component, the peak at more negative potential (peak I) and the peak at more positive potential (peak III) correspond to the transfer of +2 charged species, since the half-peak width equals 45 mV; whereas the peak at the center (peak II) corresponds to the transfer of a +3 charged species, as its half-peak width is 30 mV. This observation is further confirmed by the dc cyclic voltammogram and absorption spectra. From these results it may be concluded that peaks I and III are due to the transfer of $[Co(terpy)_2]^{2+}$ and $[Co(terpy)]^{2+}$, respectively. The mono ligand complex (peak III) is expected to be more strongly solvated in water than its diligand analogue and thus to transfer at a more positive potential. Peak II corresponds to the oxidation of either Co^{2+} to Co^{3+} or $[Co(terpy)_2]^{2+}$ to $[Co(terpy)_2]^{3+}$.

The transfer of the terpyridine complexes of Ni^{2+}, Zn^{2+}, and Cu^{2+} for a metal:ligand concentration ratio of 5:1 is shown in Figure 6. The peaks which appear in the positive potential region are due to the transfer of the monoligand complexes, whereas the peaks in the negative region correspond to the diligand complexes.

All the transfer processes exhibit diffusion-controlled reversible behaviour. It is seen that the Ni^{2+} complexes show predominantly the transfer of $[Ni(terpy)_2]^{2+}$ complex, while the $[Ni(terpy)_2]^{2+}$ appears as a shoulder even though the complexes were prepared from an excess amount of Ni^{2+} ions. On the other hand, the transfer of the Zn^{2+} complex shows the opposite behaviour, with a relatively larger transfer peak of $[Zn(terpy)]^{2+}$ than that of $[Zn(terpy)_2]^{2+}$. The transfer peak of the Cu^{2+} complex is completely dominated by $[Cu(terpy)]^{2+}$, with a peak current density which is three times that of $[Zn(terpy)]^{2+}$. The relative stability of the complexes may be inferred from the corresponding peak current densities; accordingly, for the monoligand complexes, the following order is observed: $[Cu(terpy)]^{2+} > [Zn(terpy)]^{2+} > [Ni(terpy)]^{2+}$. For the diligand complexes, the order is $[Ni(terpy)_2]^{2+} > [Zn(terpy)_2]^{2+} > [Cu(terpy)_2]^{2+}$. This order is in fair agreement with reported values [22] with the exception of the reversed order of the monoligand com-

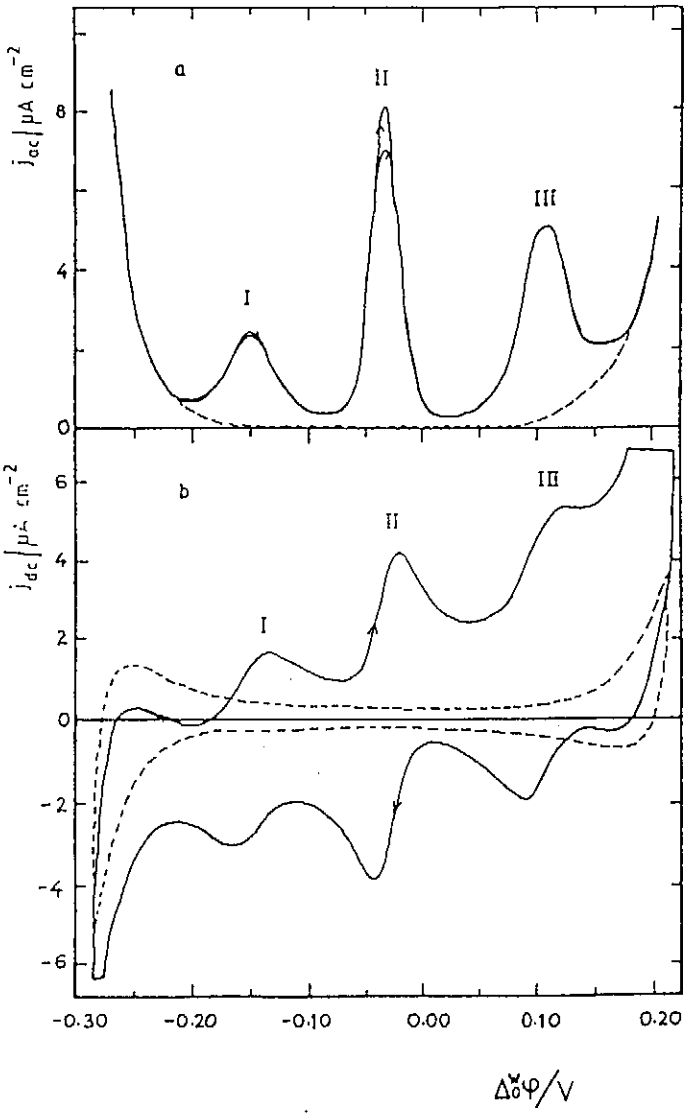

Fig. 5 Ac cyclic voltammogram of the in-phase component (a), dc cyclic voltammogram (b) and the voltammograms of the supporting electrolyte (— — —) in the water/nitrobenzene system. Air saturated aqueous solution containing 0.5 mM Co^{2+}, 0.1 mM terpyridine, + 5 mM Li_2SO_4 as a supporting electrolyte, and 10 mM PNPDCC dissolved in nitrobenzene. f = 20 Hz, ac sweep rate = 10 mV s^{-1}, dc sweep rate = 25 mV s^{-1}, pH = 6.5

plexes of Ni^{2+} and Zn^{2+}.

The experimental thermodynamic parameters of the complex ions are given in Table III. It is interesting to note that the ΔG_t° values of the diligand complexes of Co^{2+}, Ni^{2+}, Zn^{2+}, and Fe^{2+} are within experimental error, equal

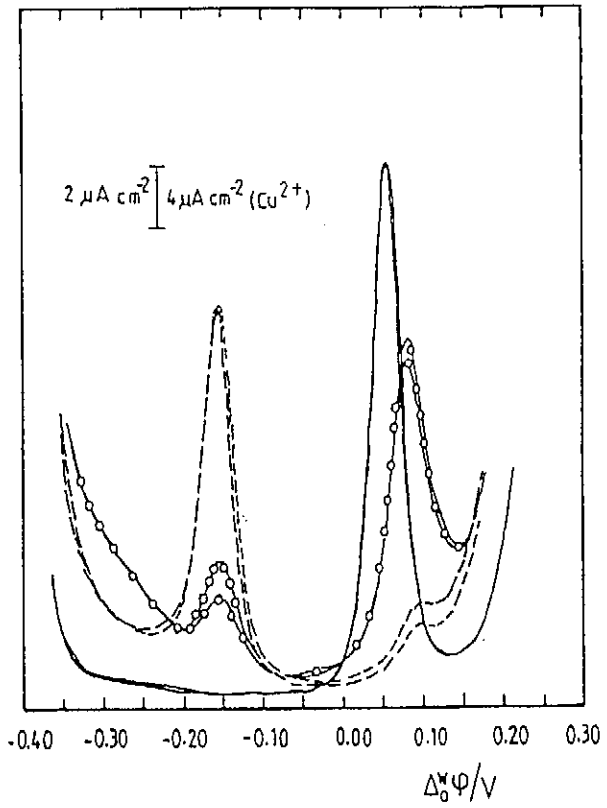

Fig. 6 Ac cyclic voltammogram for the transfer of Cu (----), Ni (-----) and Zn (-o-)-terpyridine complexes across the water/nitrobenzene interface. Aqueous solution containing 0.5 mM M^{2+} (M^{2+} = Cu^{2+}, Ni^{2+} or Zn^{2+}) and 0.1 mM terpyridine + 5 mM Li_2SO_4. Organic phase: 10 mM PNPDCC. Sweep rate = 5 mV s^{-1}, f = 20 Hz

to each other (-29 to -31 kJ mol^{-1}), and hence independent of the nature of the central metal ion. The same holds for the diligand complexes of Co^{3+} and Fe^{3+} (-11 kJ mol^{-1}).

There appears to be linear relationship between the standard Gibbs energy of transfer values and the number of pyridyl units in the complex, as shown in Fig. 7 for the Ni-bipyridine and Ni-terpyridine complexes.

For the former, the values reported by Homolka and Wendt [10] were taken. Extrapolation of the linear plot to zero ligand (i.e., for the uncomplexed Ni^{2+} ion) leads to a value of approximately 70 kJ mol^{-1} for the standard Gibbs energy of transfer of Ni^{2+} across the water/nitrobenzene interface. The present method of extrapolation may thus provide an estimate of the ΔG_t^o values for ions that transfer across an interface at potentials that fall well beyond the available potential window for given solvent systems.

Table III Diffusion coefficients in water (D_w), half-wave potentials ($\Delta^w{}_o\Phi_{1/2}$), standard Galvani potential differences ($\Delta^w{}_o\Phi^o$) and standard Gibbs energies of transfer from water to nitrobenzene ($\Delta G_t^{o(w\to o)}$) of metal-terpyridine

Complex ion	$D_w \times 10^{-6}$ $cm^2\ s^{-1}$	$\Delta^w{}_o\Phi_{1/2}$ V	$\Delta^w{}_o\Phi^o$ V	ΔG_t^o kJ mol^{-1}
$[Co(terpy)]^{2+}$	7.8	0.108	0.103	20
$[Ni(terpy)]^{2+}$	8.1	0.100	0.094	18
$[Zn(terpy)]^{2+}$	7.6	0.084	0.078	15
$[Cu(terpy)]^{2+}$	7.8	0.056	0.051	10
$[Co(terpy)_2]^{2+}$	4.0	-0.150	-0.155	-30
$[Ni(terpy)_2]^{2+}$	5.3	-0.154	-0.160	-31
$[Zn(terpy)_2]^{2+}$	5.3	-0.156	-0.162	-31
$[Cu(terpy)_2]^{2+}$	3.8	-0.144	-0.149	-29
$[Fe(terpy)_2]^{2+}$	4.0	-0.148	-0.152	-29
$[Co(terpy)_2]^{3+}$	5.0	0.033	-0.037	-11
$[Fe(terpy)_2]^{3+}$	5.1	-0.032	-0.038	-11

(iii) Flow Injection Analysis of Ion Transfer across the Membrane Stabilised Interface of Two Immiscible Electrolyte Solutions.

When a lipophilic poly(ethylene terephthalate) membrane is employed to stabilise the water/nitrobenzene interface, the void volume of the membrane will be filled by the organic phase and the interface is formed at the membrane surface directed toward the aqueous phase. Thus the potential-current curve for the diffusion-controlled ion transfer from water to nitrobenzene can be described by the Nicholson–Shain theory [23]. The voltammogram for the transfer of the ClO_4^- from water to nitrobenzene was recorded (not shown) in a quite solution. The area A of the interface was calculated from the peak current, i_p, using the relation

$$A = \frac{i_p}{268.7\, c (D\nu)^{1/2}} \qquad (2)$$

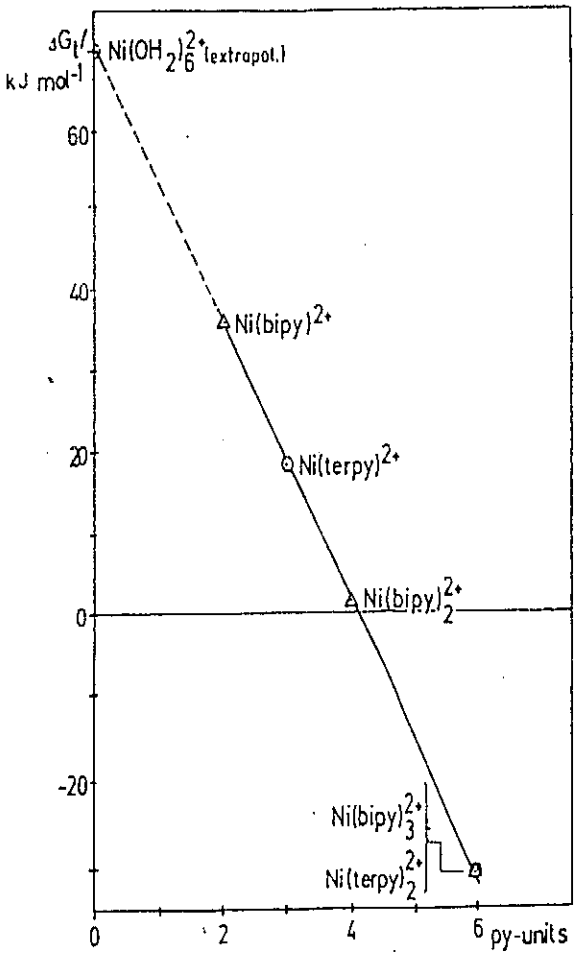

Fig. 7 $\Delta G_t^{o(w\to o)}$ of Ni-terpyridine complexes vs. the number of pyridyl units

Taking the diffusion coefficient of ClO_4^- in water as 1.8×10^{-5} cm^2 s^{-1}, the active area of the interface evaluated in this way was found to be 0.37 cm^2, a value in very good agreement with the geometrical area of the interface (0.38 cm^2). Thus, it can be assumed that the aqueous side of the membrane is covered by a thin film of the organic phase. It was observed from the voltammograms obtained that the limiting diffusion current, which is inversely proportional to the stagnant diffusion layer δ, depends on the volume flow rate ν. When the Galvani potential difference across the membrane stabilised interface is kept constant within the polarization range, the concentration of the ion under study in the bulk solution will correspond to the concentration gradient of the ion at the interface, and subsequently to the current monitored. If the concentration changes in the bulk solution are much slower than the diffusion controlled response dynamics of the sensor, the concentration gradient at the interface may

be described by $(C - C_{x=0})/\delta$. Introducing a limiting current, i_l, obtained at Galvani potential differences where $C_{x=0}$ is much less than C, the relationship between current and Galvani potential difference of the transfer of an ion from water to the organic phase is given by

$$\Delta^{w}{}_{o}\Phi = \Delta^{w}{}_{o}\Phi_{1/2} - \frac{RT}{zF}\ln\left(\frac{i_l}{i} - 1\right) \tag{3}$$

Figure 8 shows the dependence of the flow injection peak current, i_p on $\Delta^{w}{}_{o}\Phi$. It can be seen from the plot that current plateau was obtained for each ion studied. The application of the detector for the quantitative determination of ions was investigated. The detection limit for perchlorate based on the 3σ-criterion was found to be 0.3 μmol l^{-1}.

When a neutral carrier is dissolved in the organic phase of the detector, the facilitated transfer of hydrophilic cations can be utilized for their determination. This is shown in Fig. 9 for the amperometric determination of K^+ with DB-18-C-6 as neutral carrier.

When the detector is applied for the determination of an ion A in the presence of interfering ions, B,C, ...,I, each ion will contribute to the current i_p, taken as the signal proportional to the concentration. Thus we may write

$$i_p = Kk\sum b_i c_i \tag{4}$$

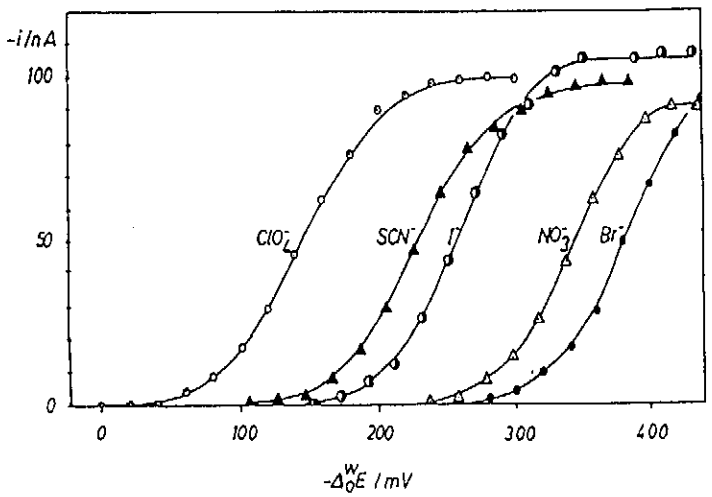

Fig. 8 Dependence of the flow injection peak height on the applied potential difference for several ions: Voltage scale $\Delta^{w}{}_{o}E = \Delta^{w}{}_{o}\Phi - 0.052$. Electrolytes: 10 mM PNPDCC in nitrobenzene, 5 mM Na_2SO_4 as carrier electrolyte and 0.1 mM analyte. Volume flow rate: 0.6 ml min^{-1} and injection volume 5 μl

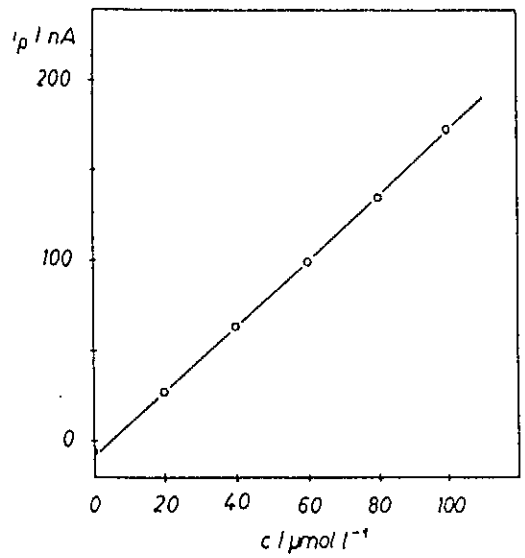

Fig. 9 Dependence of the peak height on the concentration of K^+ in the injected sample: Electrolytes - 10 mM PNPDCC + 10 mM DB-18-C-6 in nitrobenzene, 10 mM $MgSO_4$ as aqueous carrier electrolyte, $\Delta^w{}_o\Phi$ = 0.30 V, sample volume and flow rate as in Fig. 8

where b_i is the partial sensitivity of the i-th ion in the sample and K is the dispersion number of the flow injection system. Since the limiting current, i_p, in Eq. (4) is given by

$$i_p = kKz_iD_i^{2/3}c_i \quad , \tag{5}$$

the partial sensitivity of an individual ion can be derived by rearrangement of Eq. (4) and is given by

$$b_i = \frac{z_iD_i^{2/3}}{\exp\left[\frac{z_iF}{RT}\left(\Delta^w{}_o\Phi_{1/2} - \Delta^w{}_o\Phi\right)\right] + 1} \tag{6}$$

It can be seen from Eq. (6) that the partial sensitivity of the detector for a certain ion is determined by the difference between the applied Galvani potential difference and the respective half-wave Galvani potential difference. Hence, from this point of view, the amperometric detector will always exhibit the highest partial sensitivity to the most lipophilic ion in the sample, like a liquid state ISE. In spite of this common drawback the amperometric detector is superior to the liquid state ISE since its selectivity is determined by quantities which can be obtained by independent experiments. (D, $\Delta^w{}_o\Phi_{1/2}$).

Thus, when the concentrations of the interfering ions can be determined by other methods, the signals can easily be corrected while the correction of the potentiometric signal is difficult due to the dependence of the potentiometric selectivity coefficient on the concentration of the primary ion in the membrane and on the concentration of the interfering ion in the sample, the former being unknown in most practical cases.

The performance of the amperometric detector in a flow injection system shows that it may be used as an alternative detector in ion chromatography.

Conclusion

The above experimental results show that ion transfer study with two immiscible electrolyte solutions is an effective electrochemical method for obtaining thermodynamic parameters such as the standard Gibbs transfer energy and analytical determination of substances that cannot be studied by the conventional electrochemical method. The stabilisation of ITIES by lipophilic or hydrophilic membranes allows the detection of ions by flow injection analysis (FIA). FIA amperometric detection at ITIES has a convenient operation and inexpensive instrumentation.

References

1. V.E. Kazarinov (Ed.), *The Interface Structure and Electrochemical Process at the Boundary Between Two Immiscible Liquids*, Springer-Verlag, Berlin 1987.
2. Koryta J.: Electrochim. Acta, **33**, 189 (1988).
3. Girault H.H., Schiffrin D.J. in *Electroanalytical Chemistry, Vol. 15*, (A.J. Bard, Ed.), Marcel Dekker, New York 1989.
4. Mareček V., Samec Z., Koryta J.: Advances in Colloid and Interface Science **1**, 29 (1988).
5. Markus Y.: Pure and Appl. Chem. **55**, 977 (1983).
6. Koryta J.: Electrochim. Acta **24**, 293 (1979); **29**, 445 (1984).
7. Mareček V., Samec Z.: Anal. Lett. **14**, 1241 (1981).
8. Koryta J., Guo D., Ruth W., Vanýsek P.: Faraday Disc. Chem. Soc. **77**, 209 (1984).
9. Sabela A., Koryta J., Valent O.: J. Electroanal. Chem. **204**, 267 (1986).
10. Homolka D., Wendt H.: Ber. Bunsenges. **89**, 1075 (1985).
11. Ross J.W.: Science **156**, 1378 (1967).
12. Osakai T., Nuno T., Yamamoto Y., Saito A., Senda M.: Bunseki Kagaku **38**, 479 (1989).
13. Hundhammer B., Dahawan S.K., Bekele A., Seidlitz H.J.: J. Electroanal.

Chem. **44**, 253 (1987).
14. Hundhammer B., Solomon T., Alemu H.: J. Electroanal. Chem. **149**, 179 (1983).
15. Bard A.J., Faulkner L.R.: *Electrochemical Methods, Fundamentals and Applications*, Wiley, New York 1980.
16. Abrham M.H., Liszi J.: J. Inorg. Nucl. Chem. **43**, 143 (1981).
17. Abrham M.H., Liszi J.: J. Chem. Soc. Faraday Trans. I. **74**, 1604 (1978).
18. Kenjo T., Diamond R.H.: J. Inorg. Nucl. Chem. **36**, 183 (1974).
19. *CRC Handbook of Chemistry and Physics*, CRC Press, Cleveland OH 1988.
20. Czapkiewicz J., Czapkiewicz-Tutaj B.: J. Chem. Soc., Faraday Trans. I, **76**, 1663 (1980).
21. Solomon T.: J. Electroanal. Chem. **313**, 29 (1991).
22. Holyer R., Hubbard C., Kettle S., Wilkins R.: Inorg. Chem. **5**, 622 (1966).
23. Nicholson R.S., Shain I.: Anal. Chem. **36**, 704 (1964).